Comprehensive Exam Document

Anthony Moeller

Part I: HF PMT Simulation

HF and High Energy Events in HF Testbeam

The CMS Hadronic Forward (HF) Calorimeter covers the pseudorapidity region of approximately $2.9 < \eta < 5$. It is composed of quartz fibers of two different lengths embedded in steel absorbers, with the PMT readout box assembly sitting behind the calorimeter at roughly $3 < \eta < 3.2$, see Figure 1. For more information on HF, see reference [1].

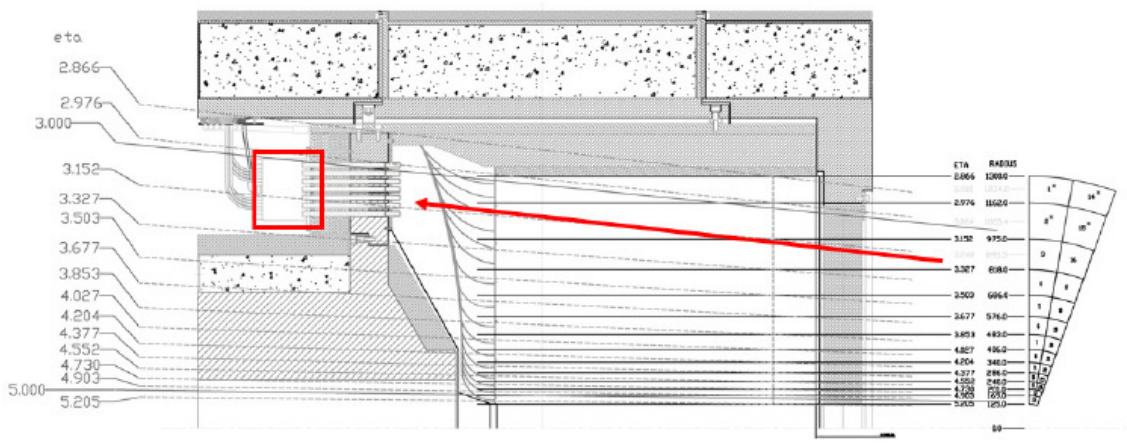

Figure 1. Diagram of HF. The red box is the PMT readout box, and the arrow indicates particles traveling from the interaction point.

Abnormally high energy events were observed during the HF testbeam in 2004. These events were present for both muon and pion beams. A handful of these high energy events were seen in electron runs, but these are likely due to beam contamination. For more information on the testbeam and analysis of these events, see references [2] and [3].

The steel absorber of HF is 165 cm long and should contain most of the hadronic longitudinal showers.However, some of the hadronic shower may leak out the back of HF. In addition, muons can pass directly through HF. When muons strike the PMT directly, or some component of the hadronic shower from pions hits the PMT, particles may pass through the PMT window. As the particles pass through the window, Cerenkov radiation is generated, and an abnormally large (equivalent to several hundred GeV) signal is registered in the PMT. For more on Cerenkov radiation in this specific geometry, see reference [2].

Simulation of PMT Events using CMSSW

To further study and verify these abnormal events, the exiting full simulation using CMSSW and Geant4 was modified. The PMT windows were added as separate sensitive detectors. The PMT windows are currently incorporated as disks of uniform

thickness (6 mm), although the windows of the PMTs currently installed on HF are plano-convex. The current window is 6 mm thick at the edges, but is much thinner in the center. Any differences in window thickness will have an impact in the distribution of Cerenkov photons produced in the windows, whether it be the difference between the real PMTs and the simulation, or with any replacement PMTs that may be used in the future [4]. The standard HF simulation utilizes shower libraries for hadronic as well as electromagnetic showers. In this approach any hadron, electron, positron or photon entering the forward calorimeter is removed and replaced by a number of photo-electrons (1 p.e. corresponds to about 4 GeV) which are obtained from a pre-generated shower kept in a library. This approach needs to be modified to take care of shower leakage in case of hadronic showers. The new approach for a parameterization of showers in HF continues to utilize the shower library for electrons, positrons, and photons. Hadrons are treated differently. The hadrons themselves are transported using Geant4, while the electromagnetic component of the hadronic showers are either transported using Geant4 or are replaced using the shower library depending on their longitudinal position within HF.

Datasets

Datasets of 100,000 particles each were generated for 100 GeV electrons, 150 GeV muons, and 100 GeV pions using a particle gun. A dataset of 100,000 jets at 50 GeV pT was generated using a particle gun like interface for Pythia. The pseudorapidity range for these datasets was $3 < \eta < 3.3$, which roughly corresponds to the position of the readout box behind HF containing the PMTs.

About 100,000 minimum bias events were generated for collision energies of 7, 10 and 14 TeV (The actual number of events varies somewhat for each energy, and can be found in Table 1).

Table 1: Number of events per dataset.

COM Energy (TeV)	No. of Events
7	96000
10	93000
14	95000

Additional datasets of about 100,000 more events for 150 GeV muons, 50 GeV pT Pythia jets, and 7 TeV minimum bias events were generated for a thinner window (0.6 mm) in order to compare the effects of changing the thickness of the window.

PMT Hits

In agreement with the data from TB04 [2], in this simulation, hits are seen in the PMTs for 150 GeV Muons (Figure 2), 100 GeV Pions (Figure 3), and 50 GeV pT Pythia jets (Figure 4). For muons, pions, and jets, there is a peak at about 50 photoelectrons. If a lower energy threshold of 12.5 photoelectrons (50 GeV) in the PMTs per event is imposed, 0.753% of pion, 17.8% of muon, and 3.70% of Pythia jet events are PMT events, where the incident particle is aimed at the PMT region, as explained earlier.

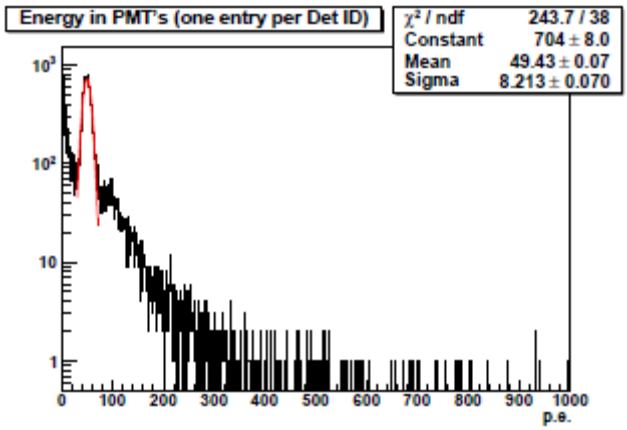

Figure 2. Energy in PMTs, 150 GeV muons.

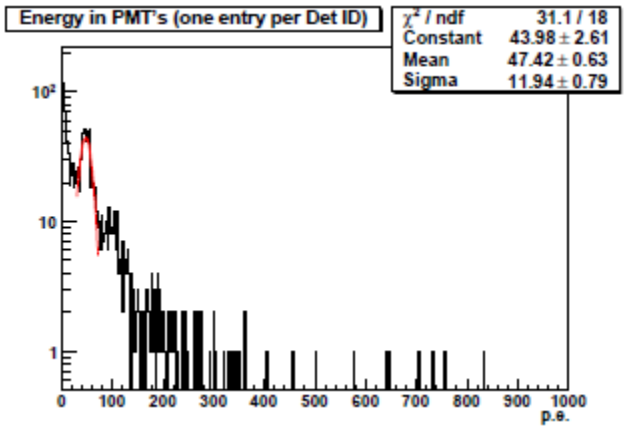

Figure 3. Energy in PMTs, 100 GeV pions.

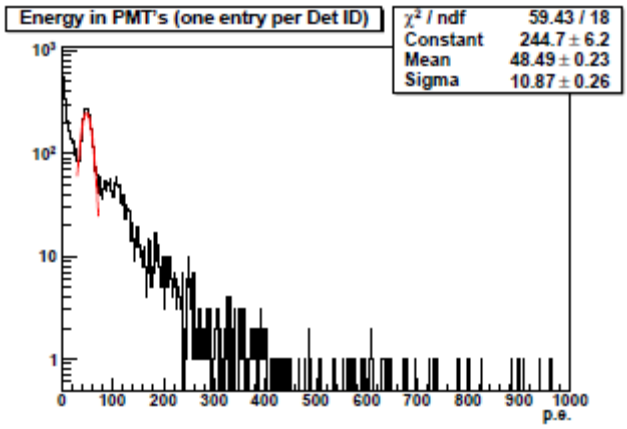

Figure 4. Energy in PMTs, 50 GeV pT Pythia jets.

For all three minimum bias datasets, a peak was also seen at about 50 photoelectrons. If a lower energy threshold of 12.5 photoelectrons (50 GeV) in the PMTs per event is imposed, 0.70% of 7 TeV, 0.85% of 10 TeV, and 0.93% of 14 TeV minimum bias events are PMT events. Note that the numbers in Figures 5, 6, and 7 indicate the

number of hits, and not the number of simulated events. These figures show only the energy deposited in the PMT windows, and do not include the energy in the long and short fibers from the body of HF.

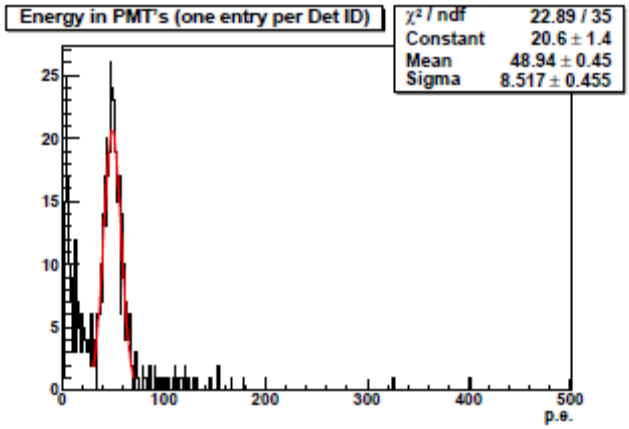

Figure 5. Energy in PMTs, 7 TeV minimum bias events.

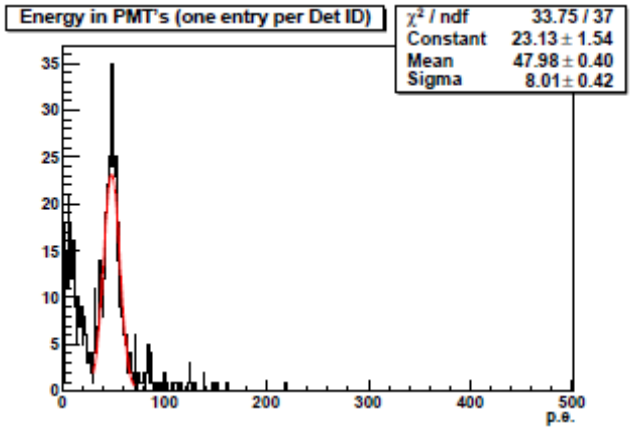

Figure 6. Energy in PMTs, 10 TeV minimum bias events.

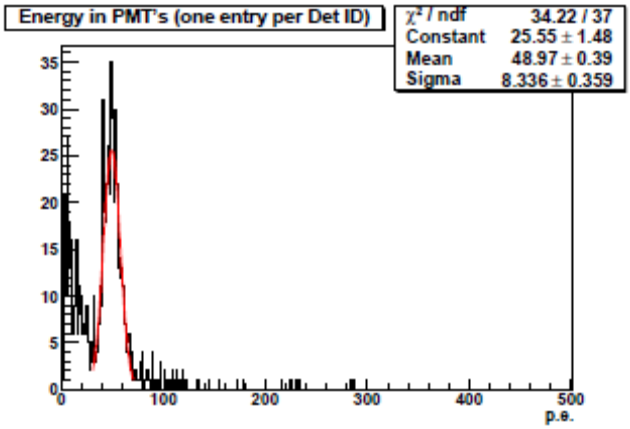

Figure 7. Energy in PMTs, 14 TeV minimum bias events.

Figures 8, 9, and 10 show the energy deposited in the PMT windows of two different thicknesses for 150 GeV Muons, 50 GeV pT Pythia jets, and 7 TeV minimum bias events, respectively. Note that these figures show only the energy deposited in the PMT windows, and do not include the energy in the long and short fibers from the body of HF. In all three cases, the location of the peak drops from about 50 p.e. for the 6 mm window to about 5 p.e. for the 0.6 mm window. For more details on the amount of Cerenkov radiation produced in the glass window, see reference [2]. If a lower threshold of 12.5 p.e. (50 GeV) is imposed, the number of PMT hits seem in muons drops quite dramatically for the thinner window (from 18.0% to 1.5%). A significant, although not as dramatic, decrease is also seen for the minimum bias events (from 0.70% to 0.37%), and Pythia jets (from 4.4% to 3.2%).

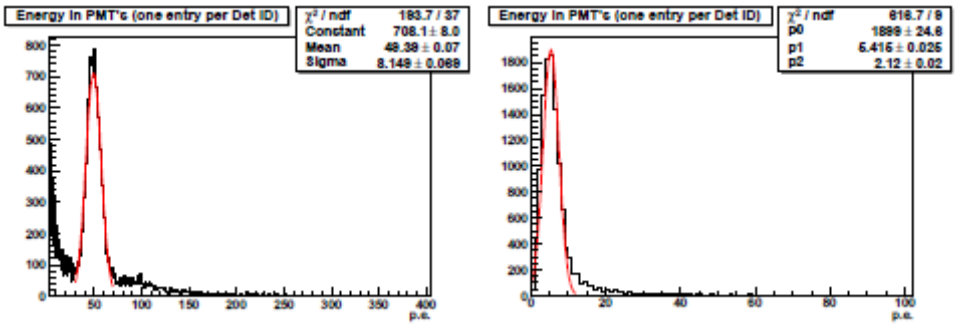

Figure 8. Energy in PMTs, 150 GeV muons, 6 mm window on left, 0.6 mm window on right.

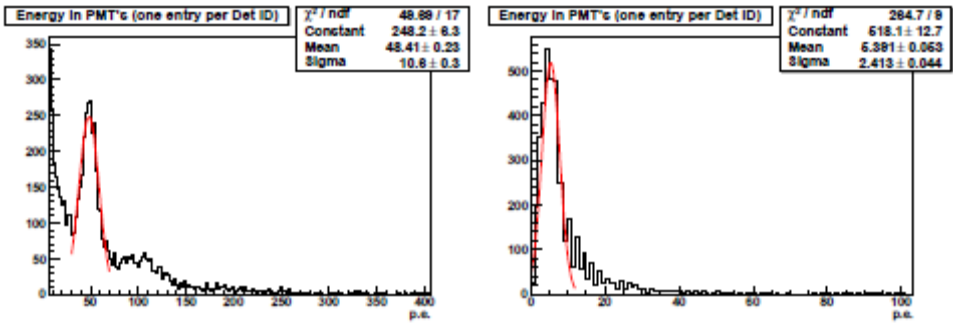

Figure 9. Energy in PMTs, 50 GeV pT Pythia jets, 6 mm window on left, 0.6 mm window on right.

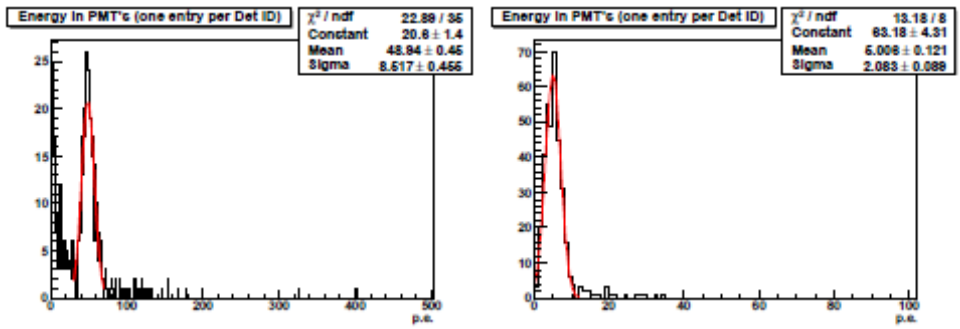

Figure 10. Energy in PMTs, 7 TeV minimum bias events, 6 mm window on left, 0.6 mm window on right.

Timing

Particles traveling through HF travel at close to the speed of light, while the signal traveling through the HF fibers travels at a reduced speed that is dependent on the index of refraction of the fiber material. This means that PMT events should occur at an earlier time than normal HF events. The energy weighted time is shown for muon, pion, jet, and minimum bias hits in Figures 11- 16, with pcalohit times on the left, and rechit times on the right. In all cases the PMT hits peak several nanoseconds before the HF body hits. Note that the time scales for pcalohits and rechits are not identical, as the pcalohit time is the time of flight from the interaction point, while such information is not available for rechit times, which have a more arbitrary time scale.

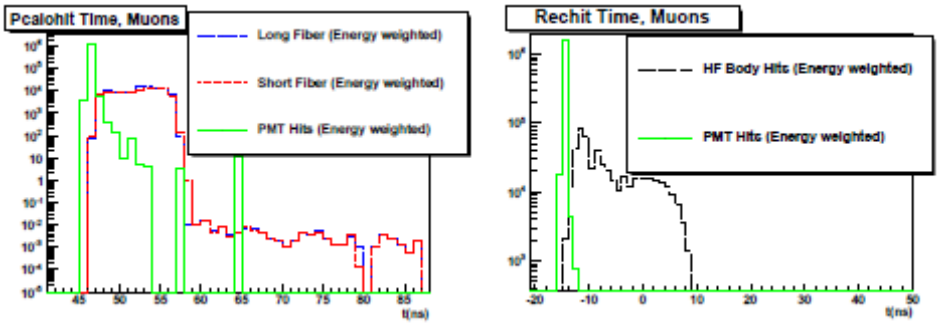

Figure 11. Timing for muons.

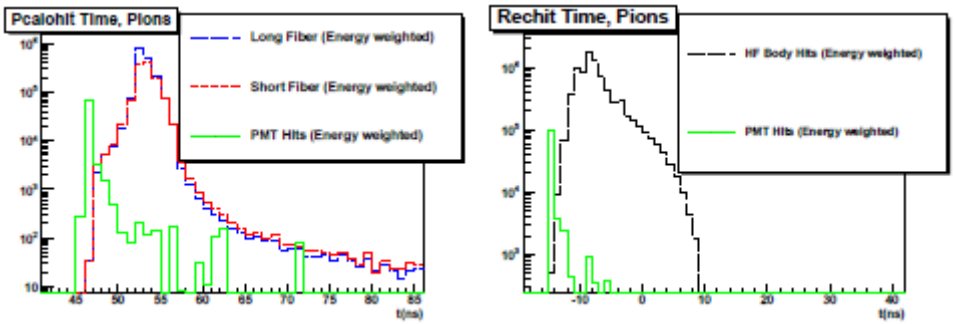

Figure 12. Timing for pions.

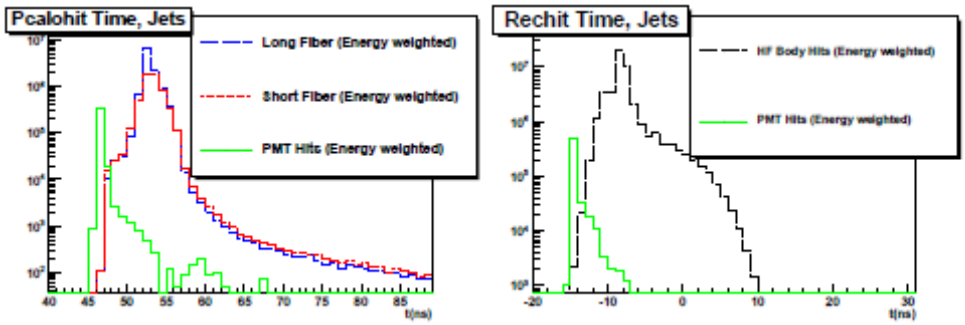

Figure 13. Timing for Pythia jets.

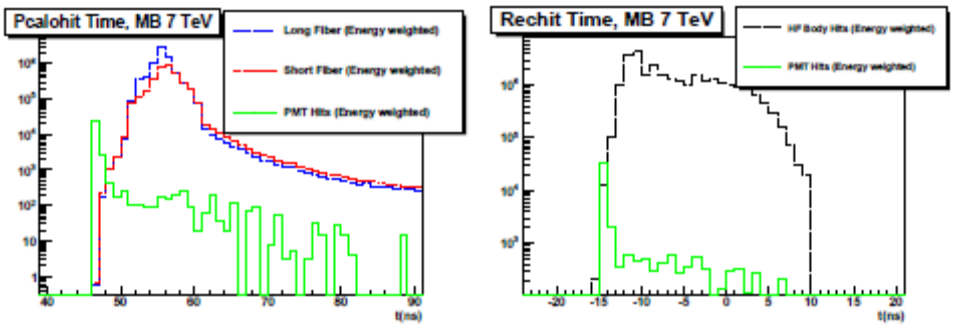

Figure 14. Timing for 7 TeV minimum bias events.

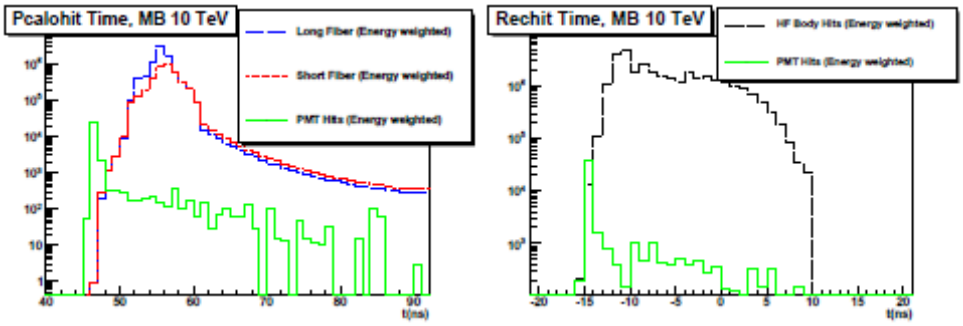

Figure 15. Timing for 10 TeV minimum bias events.

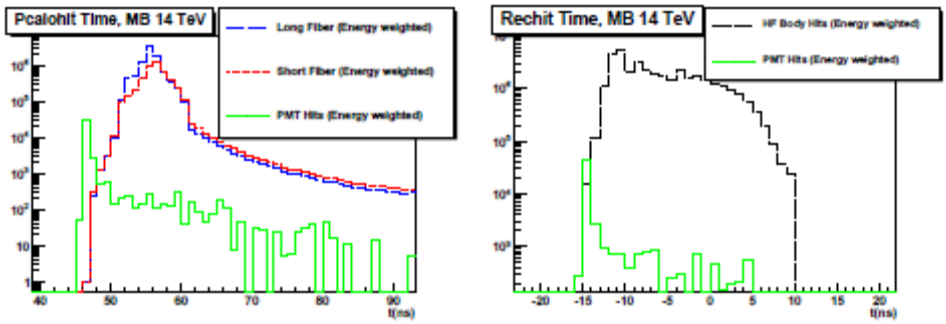

Figure 16. Timing for 14 TeV minimum bias events.

Acknowledgments

While in progress this work was regularly presented at Calorimetry Task Force meetings at the Fermi National Accelerator Laboratory. I would like to thank the members of this task force for their invaluable feedback.

References

[1] CERN-LHCC-2006-001, G.L. Baiatian et al., CMS Physics TDR: Volume I (PTDR1), Detector Performaceand Software.

[2] CMS IN 2008/014, A. Moeller, et al., Analysis of Abnormally High Energy Events in CMS Forward Calorimeters (2008).

[3] CMS Note 2006/044, S.Abdullin et al., Design, Performance, and Calibration of CMS Forward Calorimeter Wedges. Published in EPJ C, Vol 53, No 1 (2008).

[4] CMS DN 2009/011, B. Bilki, et al., Tests of CMS HF Candidate PMTs with Muons (2009).

Part II: Mass Reconstruction Methods for qqH, H→ττ→Leptonic Decay

(Note that figure numbering restarts at 1)

Introduction

The Large Hadron Collider (LHC) Experiment will provide the opportunity to investigate physics at higher energy ranges than ever before. One potential discovery is the Standard Model Higgs Boson, whose existence would help explain electroweak symmetry breaking.

While gluon fusion processes may be dominant in the production of the Higgs Boson, the vector boson fusion process has a larger discovery potential due to forward jets. Acceptance or rejection of events based on the presence of forward jets is one of the most effective tools in eliminating background events[1].

The decay H→ττ has a branching ratio of about 8% forM_H<135GeV [1], and is thus an interesting channel in the relatively low mass range.

There are CMS analyses which deal with the VBF H→ττ channel, see [2] and [3]. The focus of these existing studies is for the final state where one τ decays hadronically, and the other decays leptonically.

While the τ decays may be hadronic or leptonic, the focus of this study is on those events where the decay of both particles is leptonic, where the leptons are either electrons or muons.

Data Set

Two data sets were used in this analysis. Monte Carlo data samples from the summer of 2008 Higgs masses of 115 and 130 GeV were used. The 115 GeV data set contains 158340 events, and the 130 GeV data set contains 124381 events.

In these data sets, the τ particles are forced to decay leptonically, therefore this data set does not contain events where the decay of one or both of the τ particles is hadronic. In reality however, the branching ratios for the τ decays must be taken into consideration. The branching ratio for decaying into an electron and two neutrinos is 17.85%, and the ratio of it decaying into a muon and two neutrinos is 17.36% [4]. Therefore the branching ratio of the τ decaying leptonically into either electrons or muons is 17.85% + 17.36% = 35.21%, and the branching ratio for both τ particles decaying leptonically is thus (0.3521)2 = 0.1240, or 12.40%. So while the number of VBF Higgs events in which both τ particles decay leptonically is not large, it is still quite significant.

The qqH→ττ →Leptons Signal

In this channel, the Higgs decays to two τ particles, each of which decays into a lepton (electron or muon) and two corresponding neutrinos. While direct access to the neutrinos is possible at the generator level in the simulated data, direct information about the neutrinos will not be accessible in real LHC data. Therefore we must look at missing transverse energy (MET) to determine the energy from the neutrinos. In this study, both generated and reconstructed MET have been used.

In addition to the final state decay products, the signal from this channel also contains forward jets, which should prove useful in distinguishing the Higgs signal from that of background processes. While most events do contain more than two jets, the jets

of interest are the forward tagging jets. To be selected as a forward jet pair, the jets were required to meet the following requirements:

1. $\eta_{j1}*\eta_{j2}< -1$
2. $\Delta\eta \geq 4.5$
3. The pT of each jet must be higher than the pT cut. pT cuts of 10, 20 and 30 GeV were imposed.

The η distribution of the forward jet pairs for all three pT cuts is shown in Figure 1.

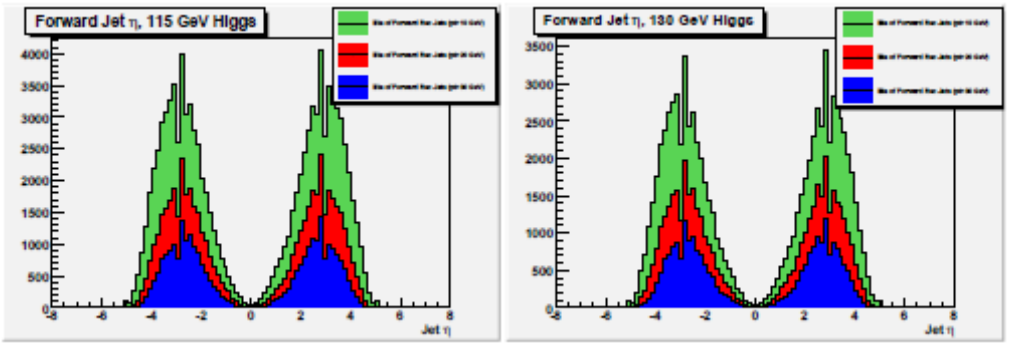

Figure 1. Angular distribution of forward jets.

Mass Reconstruction Methods

According to Rainwater and Zeppenfeld [5], the mass of the Higgs can be determined using a collinear approximation. In this approximation, the mass of the Higgs can be constructed if two quantities are known. The first quantity required is the mass of the final state leptons (muons or electrons). The second quantity is the fraction of the τ 's momentum that is carried by the neutrinos. With these quantities, the mass of the Higgs is given by $M_H \approx M_{ll}/\sqrt{(X_1X_2)}$, where M_H is the mass of the Higgs, M_{ll} is the final state mass of the leptons, and X_1 and X_2 are the fractions of each τ momentum carried by their corresponding neutrino pairs.

In addition, the neutrinos should be relatively close to their corresponding leptons in eta/phi space. As seen in Figure 2, the separation between leptons and neutrinos is generally quite small (on the order of a couple degrees), although a few events do have a significantly larger angle. A small separation between the neutrinos and the leptons implies that by knowing the direction of the leptons, the direction of the neutrinos (and thus the MET) is known, and thus for the purposes of this study, that the direction of the particles is known. This allows the construction ofthe Higgs invariant mass, as opposed to just the transverse mass.

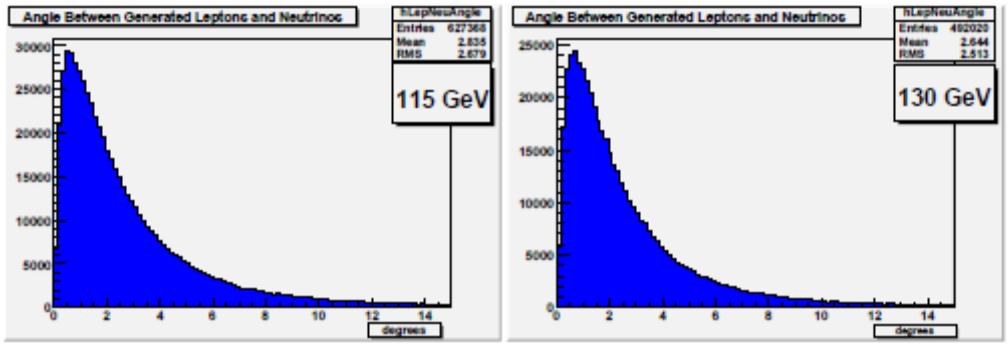

Figure 2. Angle (in degrees) between generator level leptons and neutrinos.
In this study two different mass reconstruction methods have been applied [7]. For the rest of this note, they will simply be referred to as Method 1 and Method 2. In the following two subsections, only generator level information is used in order to establish the methods. Reconstructed Higgs masses using detector level reconstructed objects will be described later in the paper.

Method 1. In Method 1, the MET in the transverse plane is calculated, with the assumption that the same momentum ratio will be valid on the z-axis as well. The neutrino pair from each τ is then treated as a single particle, using the above information to calculate a mass for each neutrino pair. The mass of the Higgs is thus the sum of the dilepton mass and the two neutrino pair masses, or $M_H = M_{ll} + M_{12} + M_{34}$, where M_{ll} is the final state mass of the leptons, and M_{12} and M_{34} are the masses of each neutrino pair. Method 1 gives a rather broad mass peak, with a mean close to the correct mass, but it has a rather large high mass tail. Reconstructed Higgs masses using generator level information are shown in Figure 3.

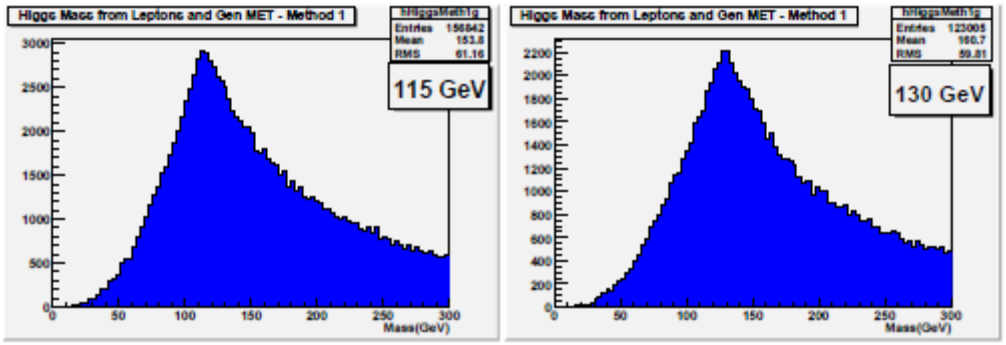

Figure 3. Mass reconstruction of Higgs using Method 1.

Method 2. Method 2 utilizes the collinear approximation formula from Rainwater and Zeppenfeld[5] to reconstruct the Higgs mass. In order to make use of this formula, it is necessary to find X_1 and X_2. In Method 2, all of the MET is added to one of the leptons in the transverse plane. Then the cross product of this quantity with the momentum of the other lepton is calculated. The ratio of the cross product of the momentum of the two leptons to the the MET added cross product is then assumed to give X. For more information on this reconstruction method, see [6].

$$X_1 = \frac{l_1.p_x \cdot l_2.p_y - l_1.p_y \cdot l_2.p_x}{l_2.p_y(l_1.p_x + \not{p}_{T\ x}) - l_2.p_x(l_1.p_y + \not{p}_{T\ y})}$$

$$X_2 = \frac{l_1.p_x \cdot l_2.p_y - l_1.p_y \cdot l_2.p_x}{l_1.p_x(l_2.p_y + \not{p}_{T\ y}) - l_1.p_y(l_2.p_x + \not{p}_{T\ x})}$$

Method 2 does give fewer events than Method 1 due to restrictions on X (since it is a fraction, it must be between 0 and 1, but there are some events where this is not true, and thus have to be rejected) but the mass peak is dramatically narrower, and the high mass tail is absent. Reconstructed Higgs masses using generator level information are shown in Figure 4.

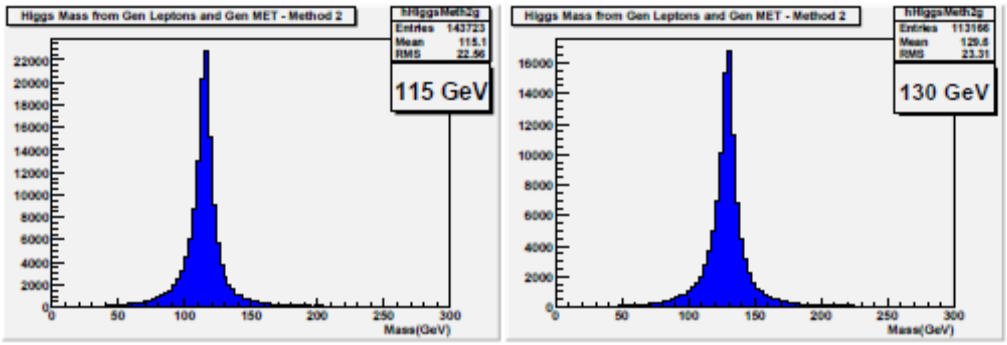

Figure 4. Reconstructed Higgs mass using Method 2.

Reconstructed Higgs Mass Using Reconstructed Leptons, Reconstructed MET, and Forward Jet Cuts

As the mass reconstruction using all generator level information for Method 2, and to a lesser extend, Method 1, look reasonable, with a clearly discernable mass peak near the generated Higgs mass for each dataset, the next step is to apply mass reconstruction to detector level reconstructed leptons and MET . Method 2 has three significant advantages over Method 1:

1. The mass peak for Method 2 is much narrower than that of Method 1.
2. Method 2 does not have the problematic high mass tail of Method 1.
3. Method 2 can be applied using only reconstructed leptons and MET , while Method 1 would require the use of reconstructed τ's.

Due to these reasons, Method 1 will be abandoned for now, and the focus will be on applying Method 2 to the reconstructed detector level objects.

Ideally, each event would contain two oppositely charged leptons, whether it be two electrons, two muons, or one muon and one electron. However, that is not the case. Mass reconstruction was only attempted on those events which had exactly one positively charged and one negatively charged lepton.

For these methods to be truly productive, these mass peaks must be able to be observed with the presence of background events. The forward jets present in this channel should be useful in reducing the background. In preparation for using the jets as a way to filter out the background, the forward jet cuts previously mentioned (See Figure 1) were applied. Figures 5 and 6 show the Higgs mass reconstruction using Method 2 using reconstructed leptons, reconstructed MET, and the forward jet cuts. Although the number of events does decrease as the threshold of the jet pT cuts increases, the overall shape is not affected greatly.

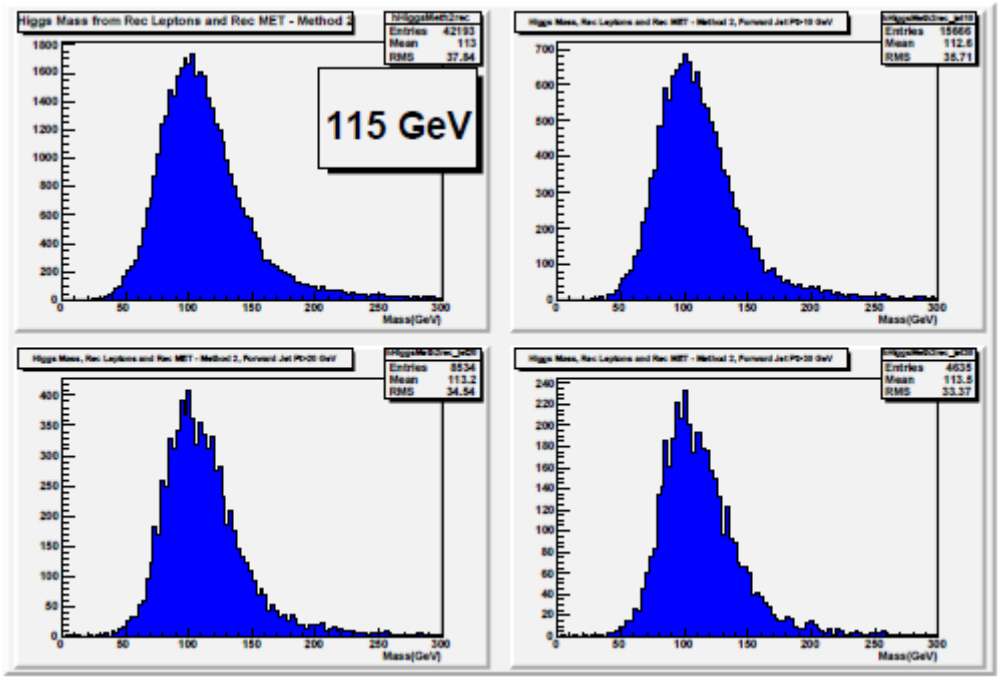

Figure 4. Results of forward jet cuts on Higgs reconstruction, 115 GeV Higgs. Top left, no cuts. The remaining histograms use the previous η cuts. Top right, jet pT>10 GeV, bottom left, jet pT>20 GeV, bottom left jet pT>30 GeV.

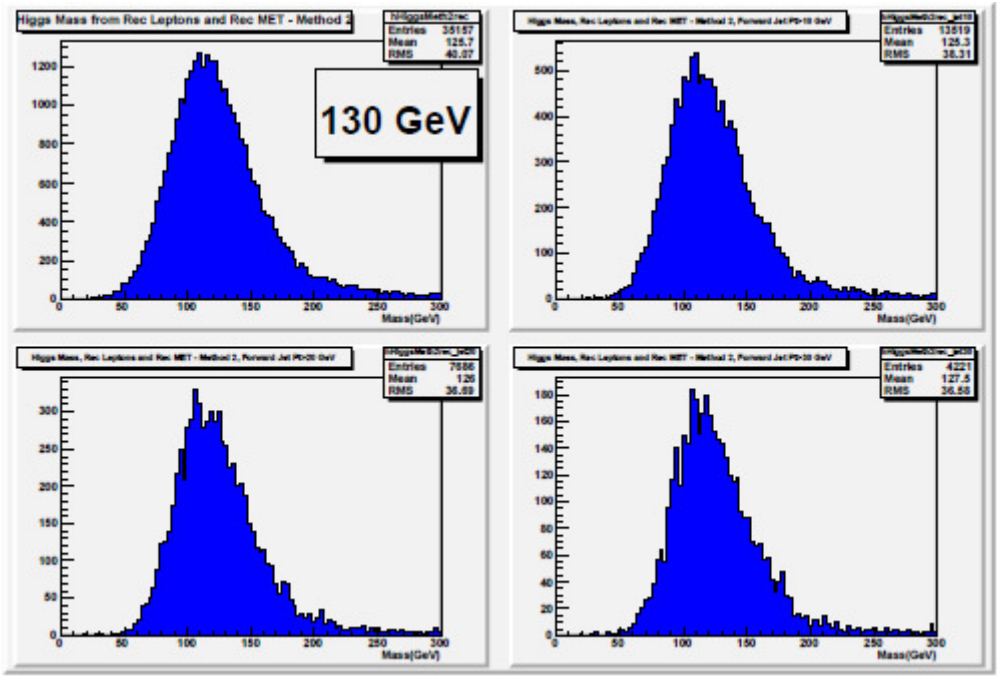

Figure 5. . Results of forward jet cuts on Higgs reconstruction, 130 GeV Higgs. Top left, no cuts. The remaining histograms use the previous η cuts. Top right, jet pT>10 GeV, bottom left, jet pT>20 GeV, bottom left jet pT>30 GeV.

Figure 6 superimposes the Higgs mass using only generator level objects and only reconstructed level objects onto the same histogram. As can be seen in these histograms, the mass peak is significantly broader when reconstructed level objects are used, and the position of the peak decreases by several GeV. The histograms are normalized to the same number of events (y axis is in arbitrary units).

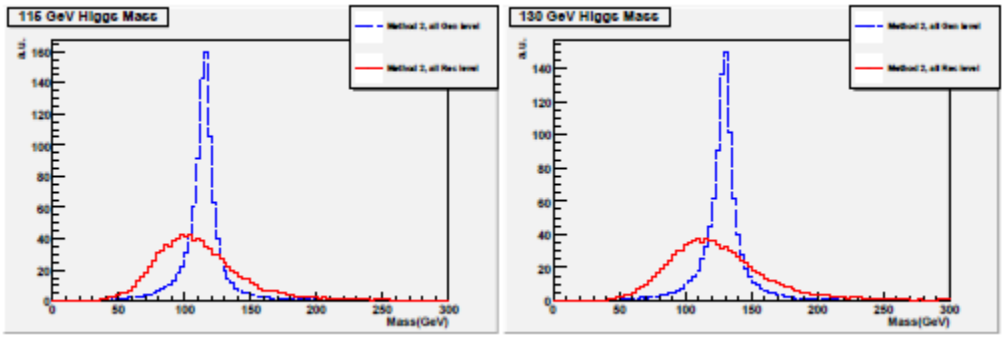

Figure 6. Mass of Higgs using Method 2, gen level and rec level results superimposed on same histogram.

Application of Method 2 to Backgrounds

The previously mentioned cuts were designed to eliminate background signals. Method 2 was applied to certain significant background channels using the same cuts applied to the Higgs datasets. The backgrounds used along with the number of events per file and the number of events remaining in each background file are shown in Table 1.

The results shown in Table 1 were used with the corresponding cross sections and branching ratios [1] to determine the number of remaining events with 30 fb^{-1} of data, see Table 2. A stack plot of these backgrounds is shown in Figure 7. The number of expected events before and after jet based cuts is also displayed as a histogram in Figure 8. As can be seen from these tables and plots, these cuts do eliminate a large fraction of the total background events, although more stringent cuts are needed as the significance is still very low (0.279 for 115 GeV and 0.205 for 130 GeV). It should also be noted that this study was also severely limited by statistically small background samples, as small background datasets were weighted based on their corresponding cross sections.

Data Set	Total Events	10 GeV p_T jet cut	20 GeV p_T jet cut	30 GeV p_T jet cut
115 GeV Higgs	158340	15666	8534	4635
130 GeV Higgs	124381	13519	7686	4221
W+Jets	9970000	510	111	43
Z+Jets	1287404	1104	96	45
Ttbar+Jets	1000000	3761	1146	529
Single Top t-channel	281756	765	299	136
Single Top s-channel	11999	12	4	1
Single Top associated W	169048	586	182	78
W+gamma	102012	29	4	0
WW+Jets	204722	196	47	20
WZ+Jets	236550	358	95	34
ZZ+Jets	199810	308	70	19
WW+2Jets (electroweak)	39299	509	347	257
WW+2Jets (VBF)	21868	558	383	245

Table 1. Number of events remaining after cuts for signal and backgrounds.

Data Set	Cross Section(pb)	10 GeV p_T jet cut	20 GeV p_T jet cut	30 GeV p_T jet cut
115 GeV Higgs	(cr. sec. x br. ratio) 0.04272	127	69	38
130 GeV Higgs	(cr. sec. x br. ratio) 0.02795	91	52	28
W+Jets	40000	61384	13360	5176
Z+Jets	3700	94329	8203	3845
Ttbar+Jets	414	46712	14233	6570
Single Top t-channel	130	10589	4139	1882
Single Top s-channel	5	150	50	13
Single Top associated W	29	3016	937	401
W+gamma	292	2.5	0.34	0
WW+Jets	74	2125	510	217
WZ+Jets	32	1453	386	138
ZZ+Jets	10.5	486	110	30
WW+2Jets (electroweak)	0.942	366	250	185
WW+2Jets (VBF)	0.41	314	215	138

Table 2. Number of events expected in 30 fb^{-1} of data.

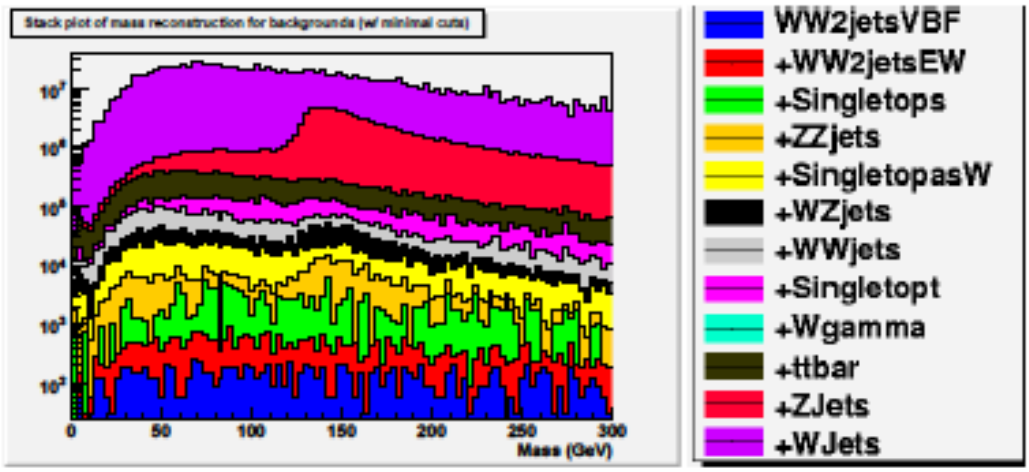

Figure 7. Stack plot showing result of mass reconstruction on backgrounds.

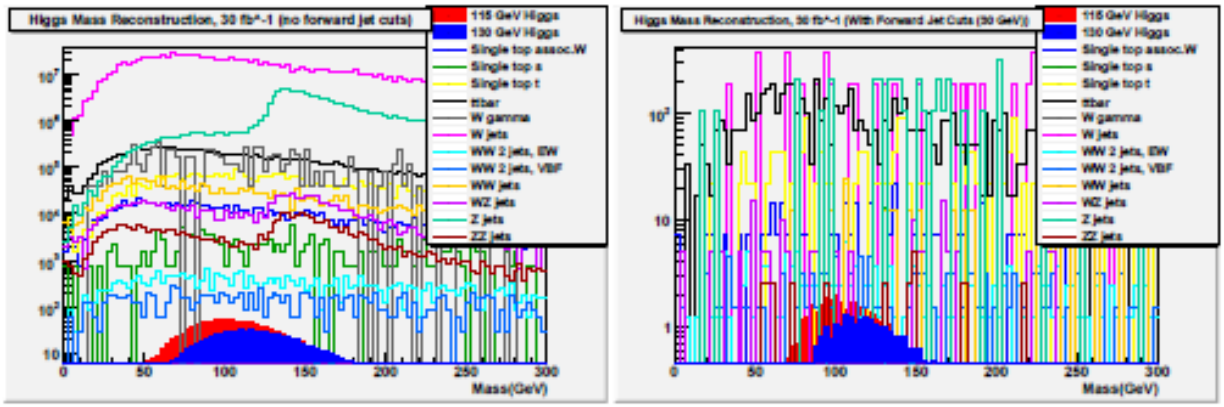

Figure 8. Reconstructed mass of Higgs and backgrounds. Minimal cuts on the left, jet based cuts included on the right.

Future Work

This study needs to be repeated with newer Monte Carlo data. The newer background samples are significantly larger, which should allow a more rigorous study of applying cuts to the backgrounds.

It should also be noted that the current amount of data from CMS is much less than the 30 fb^{-1} used in this study, and that with the current amount of data available, approximately 0 events are expected in this channel. With more data however, the use of forward jet tagging means that this channel could be interesting in the future. For the time being however, this mass reconstruction method should be applied to the Z in order to validate the method.

This method should also be applied to data to look for the Higgs as a matter of completeness, although as already mentioned, no Higgs events are likely to be found with the amount of data expected in the near future.

Acknowledgments

In addition to those mentioned in the author list, comments and suggestions from Pietro Govoni (Universita and INFN Milano-Bicocca) and Andrey Korytov (University of Florida) were crucial to the work presented in this note.

References

[1] CMS Collaboration, Physics Technical Design Report, Vol. II, LHCC 2006/021.

[2] CMS Collaboration,"Towards the Search for the Standard Model Higgs boson produced in Vector Boson Fusion and decaying into a τ pair in CMS with 1 fb^{-1}: identification studies", CMS PAS CMS PAS HIG-08-001 (2009).

[3] CMS Collaboration,"Search for the Standard Model Higgs boson produced in Vector Boson Fusion and decaying into a τ pair in CMS with 1 fb^{-1}", CMS PAS CMS PAS HIG-08-008 (2009).

[4] C. Amsler et al. (Particle Data Group), Physics Letters B667, 1 (2008).

[5] T. Plehn, D. L. Rainwater, D. Zeppenfeld, A Method for identifying $H\rightarrow\tau\tau\rightarrow e\mu pT$ at the CERN LHC., Phys. Rev. D 61, 093005, 2000.

[6] A. Collaboration, G. Aad, E. Abat, B. Abbott, J. Abdallah, A. A. Abdelalim, A. Abdesselam, O. Abdinov, B. Abi, M. Abolins, H. Abramowicz, B. S. Acharya, D. L. Adams, T. N. Addy, C. Adorisio, P. Adragna,T. Adye, J. A. Aguilar-Saavedra, M. Aharrouche, S. P. Ahlen, F. Ahles, A. Ahmad, H. Ahmed, G. Aielli, T. Akdogan, T. P. A. Akesson, G. Akimoto, M. A. Alam, S. M. Alam, J. Albert, S. Albrand, M. Aleksa, I. N. Aleksandrov, F. Alessandria, C. Alexa, G. Alexander, G. Alexandre, T. Alexopoulos, M. Alhroob, G. Alimonti, J. Alison, M. Aliyev, P. P. Allport, S. E. Allwood-Spiers, A. Aloisio, R. Alon, A. Alonso, J. Alonso, M. G. Alviggi, K. Amako, P. Amaral, C. Amelung, V. V. Ammosov, A. Amorim, G. Amoros, N. Amram, C. Anastopoulos, Anders, K. J. Anderson, A. Andreazza, V. Andrei, M. L. Andrieux, and X. S. Anduaga,
"Expected performance of the atlas experiment - detector, trigger and physics,"Dec 2008. [Online]. Available: http://arxiv.org/abs/0901.0512.

[7] Firdevs Duru, "R and D Studies On the Hadronic Calorimeter and Physics Simulations on the Standard Model and Minimal Supersymmetric Standard Model Higgs Bosons in the CMS Experiment" (PhD Thesis, University of Iowa, 2007), 119-125.